A Efficient System based on Model Segmentation for Weld Seam Grinding Robot

Jimin Ge
Hunan University of Science and Technology
Zhaohui Deng (edeng0080@vip.sina.com)
Hunan University of Science and Technology
Zhongyang Li
Hunan University of Science and Technology
Wei Li
Hunan University of Science and Technology
Tao Liu
Hunan University of Science and Technology
Hua Zhang
Hunan University of Science and Technology
Jiaxu Nie
ZOOMLION Heavy Industry Science &Technology Co., Ltd.

Research Article

Keywords: Robot, weld seam extraction, model segmentation, automatic grinding system

Posted Date: November 3rd, 2021

DOI: https://doi.org/10.21203/rs.3.rs-1043038/v1

A efficient system based on model segmentation for weld seam grinding robot

Jimin Ge[1], Zhaohui Deng[1*], Zhongyang Li[1], Wei Li[1], Tao Liu[1], Hua Zhang[1,3], Jiaxu Nie[4]

Abstract

Uneven surface quality often occurs when butt welds are manually grinding, so robotic weld grinding automation has become a fast-developing trend. Weld seam extraction and trajectory planning are important for automatic control of grinding process. However, most of the research on weld extraction is focused on before welding. Due to the irregular shape of the weld after welding, and too little work has been devoted to the weld identification after welding. Consequently, in this paper, a novel simple and efficient weld extraction algorithm is proposed, and the robot grinding path is planned. Firstly, a new flexible bracket structure for welding seam extraction is designed. Secondly, the weld seam section profile model is established, and the processing of spatial point cloud problem is transformed into the processing of two-dimensional point cloud problem. The least square method (LSM) based on threshold comparison is used to segment the weld seam, which greatly improved the processing speed and accuracy. Then the grinding path and pose are obtained according to the extracted weld space structure. Finally, a robotic welding seam automatic grinding system is built. Experiments show that the proposed method could well extract the irregular weld contour after welding and the grinding system built is reliable, which greatly improves the grinding efficiency.

Key words Robot; weld seam extraction; model segmentation; automatic grinding system

1. Introduction1

The welding technology plays an irreplaceable role in shipbuilding, automobile, aerospace and other fields [1,2]. However, welding stress will be generated in the weld area after welding, which greatly reduces the connection strength between the workpiece. The welding stress can be reduced and the fatigue strength of the workpiece can be improved by grinding the weld seam [3,4]. Therefore, it has very important practical value and significance to grind the weld after welding. At present, the grinding process for weld seam is usually done by workers, who have to endure the dust and noise. With the development of industrial technology, robotic grinding becomes widespread in high-tech industries, such as aerospace and energy because of its open and complex kinematic chain [5,6].

Nowadays, the CAD off-line programming and manual teaching are still the two main working modes of robots [7,8]. However, the manual teaching mode can not adapt to the change environment, which may lose efficacy when grinding the large and weak-stiffness welding workpieces, especially the large structural parts such as pump truck bodies and high-speed rail bodies. Therefore, in order to meet the requirements of automatic welding seam grinding of structural parts in engineering machinery, aerospace and other manufacturing fields, the development of the intelligent grinding robot is necessary that could well adapt to environmental changes.

Weld identification and trajectory planning are the core of the intelligent grinding robots, and robot sensor is the key part to realize the weld identification and trajectory planning. At present, various sensors are widely used in grinding robot, such as vision sensors [9-10], laser sensors [11],

Zhaohui Deng (✉)

Email: edeng0080@vip.sina.com

1. Hunan Provincial Key Laboratory of High Efficiency and Precision Machining of Difficult to Machine Material, Hunan University of Science and Technology, Xiangtan, 411201, Hunan, China.
2. Hubei Key Laboratory of Mechanical Transmission and Manufacturing Engineering, Wuhan University of Science and Technology., Wuhan 430000, Hubei Province, China.
3. ZOOMLION Heavy Industry Science &Technology Co., Ltd. Changsha 410000, Hunan Province, China.

force sensor [12-13], acoustic emission sensors [14], etc. Visual sensors are widely used because of their advantages of high accuracy, which are usually divided into two categories: passive vision sensors and active vision sensors [15]. Among them. Passive vision uses cameras to capture the welding seam under natural light, which can detect not only the weld seam feature but also the position deviation of weld seam. Numerous published studies apply passive vision technique for weld seam tracking [16-20], such as XU [19] designed a set of special vision sensor system for seam tracking and proposed a new improved Canny edge detection algorithm, which has worked very well. However, image of welding seam collected by this method are often disturbed by dust, arc and spatter, which increases the error of image processing.

Structured light vision is the representative of active vision, which include laser structured light [21]and encoded structured light [22]. Encoded structure light is mainly used for 3D reconstruction of workpiece and machining path planning, such as YANG [22] proposed 3D seam extraction of different weld seam based on encoded structured light to plan welding tasks. However, it is difficult to guarantee the welding efficiency and to apply to actual weld tracking because of its high requirements on environment. Therefore, it is less used in grinding. Laser structured light is usually used to extract and track the weld contour in the form of laser emitter and monocular camera. There are a variety of shapes of the laser stripe, including linear [23], multi-linear [24], a cross [25], a triangle [26], etc. SHAO [24] designed three different wavelengths of laser to measure the seam width, seam center, and the normal vector of the weld face, and the result of experiment revealed that the proposed method could meet the precision demand of space narrow butt joint. ZHANG [25] proposed a weld line localization approach for mobile platform via cross structured light, the approach could effectively reduce the influence of illumination and noise. But the laser structured is local-type sensor and it can not perceive the global range. Some scholars use three-dimensional(3D) coordinate scanner and binocular camera to obtain the global contour. But the above methods have a series of problems, such as complex algorithms, large amount of data processing and high cost, and it is still a difficult problem to accurately extract the weld parameters (width and height) from the 3D weld profile [27]. At present, the measurement-processing system for welding seam grinding is still immature. On the one hand, due to the irregular shape of the weld after welding, on the other hand, due to the complexity of the grinding process.

In view of the problems in the above research, this work investigates the method of weld feature extraction and grinding path planning with unequal thickness steel plate as the research object. (1) The weld extraction and grinding system was designed and built. (2) A simple and effective three-dimensional extraction method of welds is proposed, which transforms the problem of processing three-dimensional data into processing two-dimensional data. The model classification method based on the least square method is used to extract weld contours, and a data buffer area is created to reconstruct the three-dimensional welds. (3) The mathematical model of the weld surface is established, and the rotation angle of the robot end posture is obtained through the obtained normal vector coordinates. Based on the acquired weld characteristics, the grinding tool point is calculated. The experimental results show that the system is reliable, the processing efficiency is increased by 50%, and the surface precision of the welded seam after grinding is high. The research results are of great significance to engineering applications.

The rest of this paper is organized as follows: Section 2 describes the design and construction of the system. Section 3 describes the weld extraction process in detail. Section 4 describes the planning process of weld grinding path and pose and the realization process of system data interaction The experimental results are described in Section 5.

Finally, the conclusions of this paper are described.

2. System configuration

2.1. system platform

To ensure the feasibility of the method, a weld seam grinding robot system platform is needed to be set up. The integrated weld extraction and grinding platform is shown in Fig. 1(a). It mainly includes three parts: industrial robot system, grinding system and laser visual system. The robot system includes manipulator, controller, teach pendant. The grinding system includes motor, frequency converter and grinding wheel. The visual system includes laser vision sensor, industrial PC and self-made flexible support.

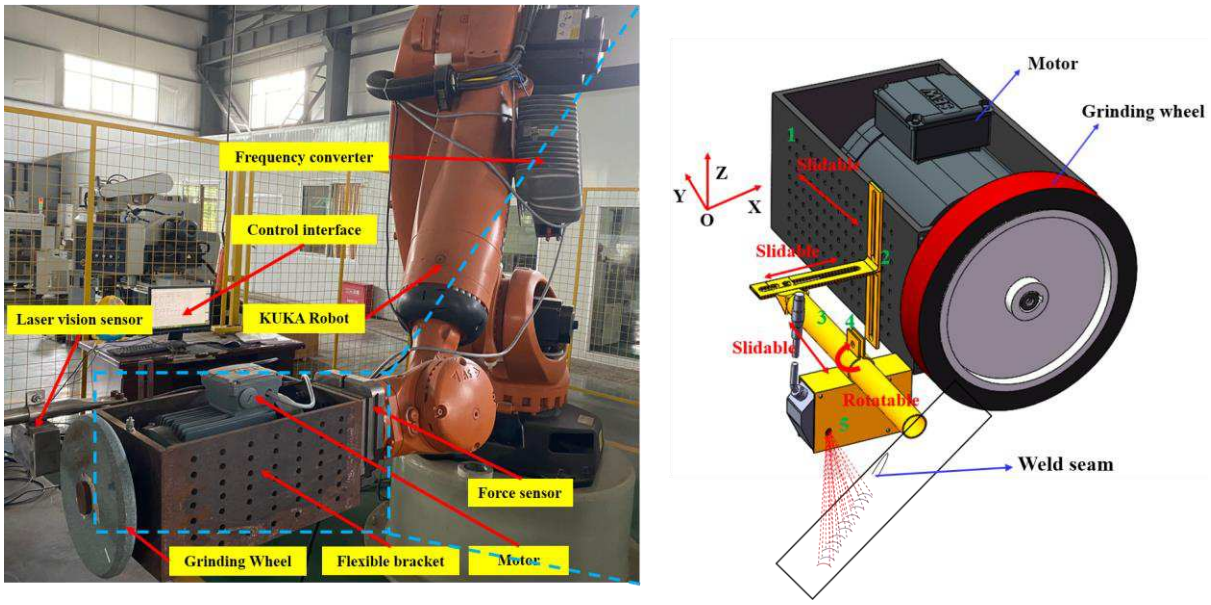

(a) weld extraction and grinding experimental platform (b) Self-made flexible bracket design

Fig.1 Experimental platform

2.2 New flexible bracket design

In order to meet processing needs, laser vision sensor and grinding system are installed at the end of the robot by a self-made flexible bracket which can ensure that the laser is projected to the surface of the weld at any angle. As shown in Figure 1(b), bracket 1 is used to install the motor and connect the grinding wheel, with regular through holes on the left. The bracket 2 is designed with 3 U-shaped grooves, which can move in the Y and z directions on the bracket 1 and ensure the movement of the bracket 3 in the x direction. The bracket 4 which fixed with bracket 5 by welding can be rotated at any angle around the bracket 3. The sensor laser head is fixed with the bracket 5 by 3 screws.

The LJ-G500 laser vision sensor developed by Keyence company is adopted, which can obtain 3D weld seam data combined with robot. And it has much advantages, such as rapid projection, high precision, high stability. At the same time, it also has small size for easy installation. Its basic parameters are shown in Table 1

It is worth noting that hand-eye calibration is performed to ensure that the robot tracks the weld seam, which essence is to obtain the transformation matrix between the sensor coordinate system and robot end coordinate system. In this paper, a high-precision mirror standard ball with a diameter of 25.4mm is used as the hand-eye calibration target. Firstly, the robot is manually controlled to move in a translational but not rotating manner to let the vision system scan the ceramic standard sphere, so that the space coordinates of the center of the sphere in the camera coordinate system is obtained. According to the constraint condition that the sphere center coordinate is invariable, the singular value decomposition is performed on the matrix to

obtain the rotation matrix part of the hand-eye matrix. Then, the robot is manually controlled to move in in any pose to let the vision system scan the ceramic standard sphere, so that the translation matrix part of the hand-eye matrix is solved by the least square method. As shown in Fig 2.

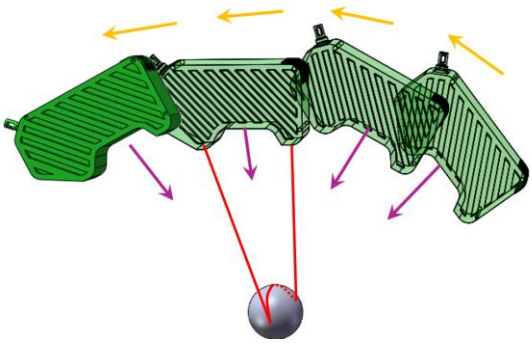

Fig.2 Hand-eye calibration

Table 1

The laser vision sensor parameters

Case	Parameters	Value
1	Accuracy	0.1%F.S
2	Sampling frequency	3.8 ms
3	Size (Length*Width*Height)	138(mm)*76(mm)*38(mm)
4	Weight	480g
5	Measuring distance	200mm

3. Method of weld seam extraction

The system built above is based on laser sensor to obtain point cloud data, and the robot pose at the same time is used to compensate for three-dimensional coordinates.

In order to accurately extract the weld seam, solve the problems of large data volume, complex algorithm and slow processing speed in traditional point cloud data processing, in this paper, the processing of three-dimensional point data cloud data is transformed into processing of two-dimensional point cloud data. For this purpose, a method based on region segmentation is proposed to extract the weld contour information of each section. The plane point cloud is firstly obtained, then the slope point cloud data is further extracted. Finally, the weld point cloud is obtained through the point cloud segmentation, and stored in the data buffer. After scanning the whole welding seam, the 3D morphology of the complete welding seam is extracted by combining the robot coordinates. Compared with processing three-dimensional point cloud data, this processing method is fast, efficient, with small data amount and guaranteed accuracy.

3.1 Model building

Unequal thickness steel plate welds are formed by butt welding two steel plates of unequal height. It is worth noting that in order to strengthen the connection strength after welding, grooves are usually processed in the area to be welded. The welding surface includes four parts: the bead, the base material (1), the base material (2) and groove area. As shown in the Fig 4, when the laser scans the weld contour, the laser line can be divided into five areas, including two planes, two bevels, and irregular weld surfaces. Therefore, point cloud data is mainly composed of plane point cloud, bevel point cloud, and weld point cloud. Considering the complexity of weld shape, it is difficult to directly establish a model to extract point cloud data. Thus, if models can be found to represent the plane area and the bevel area respectively, then weld data can be used as outliers to segment the weld profile.

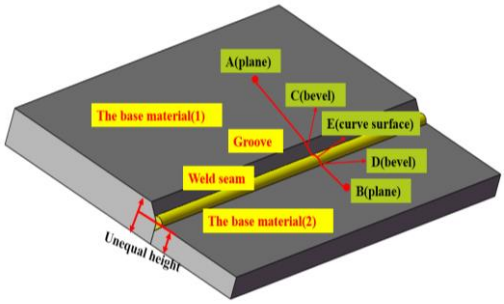

Fig.3 Weld surface profile model

According to the above analysis, the laser cloud data are orderly arranged on the basis of A-C-E-D-B region. In Butt welding, the base metal in a certain area on both sides of the weld is considered to be ideal flat. The region (A, C, D, B) can be represented by a first order polynomial respectively.

$$\begin{bmatrix} y_{Ai} \\ y_{Ci} \\ y_{Di} \\ y_{Bi} \end{bmatrix} = \begin{bmatrix} a_A \\ a_C \\ a_D \\ a_B \end{bmatrix} \mathrm{g}x_i + \begin{bmatrix} b_A \\ b_C \\ b_D \\ b_B \end{bmatrix} \tag{1}$$

Where $(y_{Ai}, y_{Ci}, y_{Di}, y_{Bi})$ are the distance between the laser sensor and the region of (A, C, D, B) at the location of x_i. x_i is laser point position, $(a_A, a_C, a_D, a_B; b_A, b_C, b_D, b_B)$ are the polynomial parameters, which can be fitted by least square method (LSM). Then the distance from the point cloud to the fitted function can be expressed as

$$d_i = y_i - y \tag{2}$$

$$(x_i, y_i) = \begin{cases} Outliers & d_i > d_S \\ Interiorpoint & d_i < d_S \end{cases} \tag{3}$$

Where y_i is the value predicted from Eq (1), y is the measured value (between the laser sensor and workpiece surface), d_S is the threshold to split the outliers.

3.2 Point cloud segmentation

Due to the data acquired by the sensor is arranged in an orderly manner by region, starting from the first point of the data, 10 points were randomly selected with a certain range and fitted by the least square method. Then the point cloud in region A was separated by Eq (1). When the continuous data was greater than the threshold value, it was considered to be region C. Then, 10 points were selected and fitted by the least square method to extract data from region C. At this moment, the starting point of the weld could be obtained.

Through the above process, regions A and C can be separated. Then search from the last point in the data, The least square method is used to fit the degree polynomial to divide the region B and D. As shown in the Fig. 4.

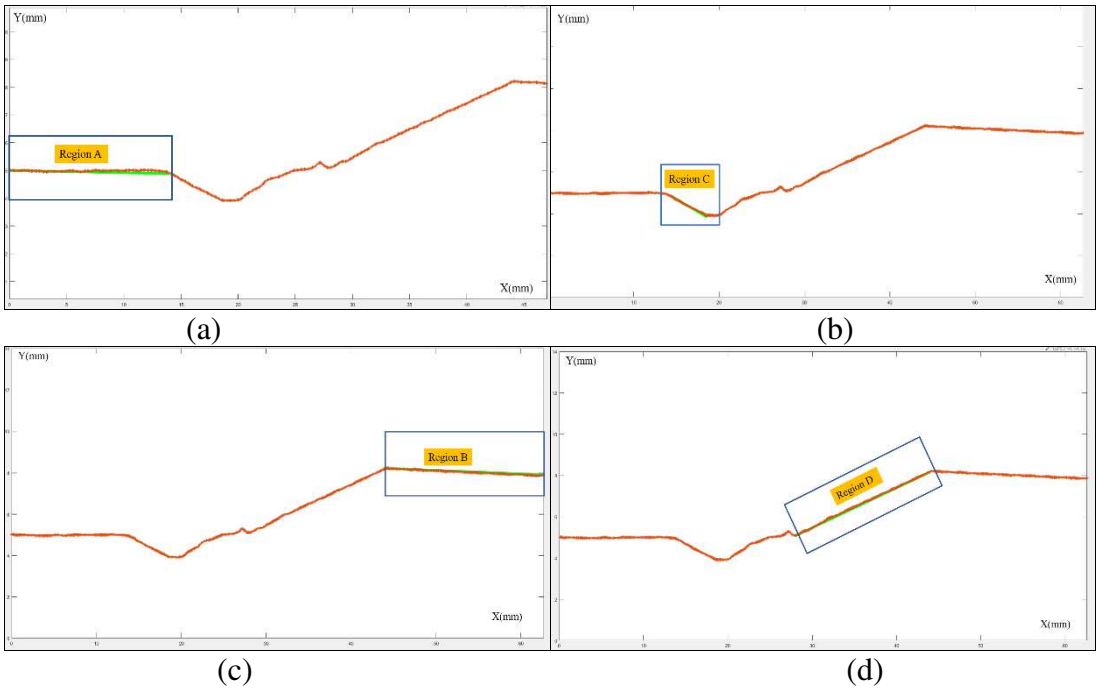

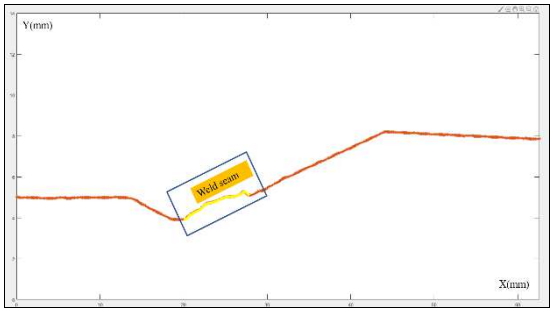

(e)

(a) extract area A; (b) extract area C; (c) extract area B; (d) extract area D; (e) extract weld.

Fig. 4 The process of weld segmentation.

After the above process, the weld profile of the section is extracted and stored in the data buffer and other point cloud data will be deleted. The 3D contour of the weld was obtained by scanning the whole weld by robot (see Fig 5).

The process of weld extraction based on model segmentation can be shown in Fig. 6

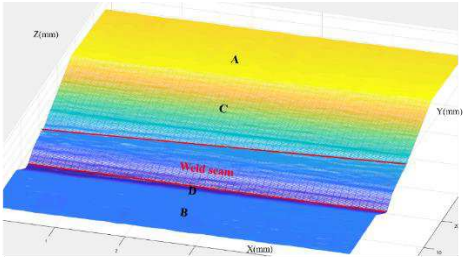

Fig. 5 Three-dimensional shape of weld

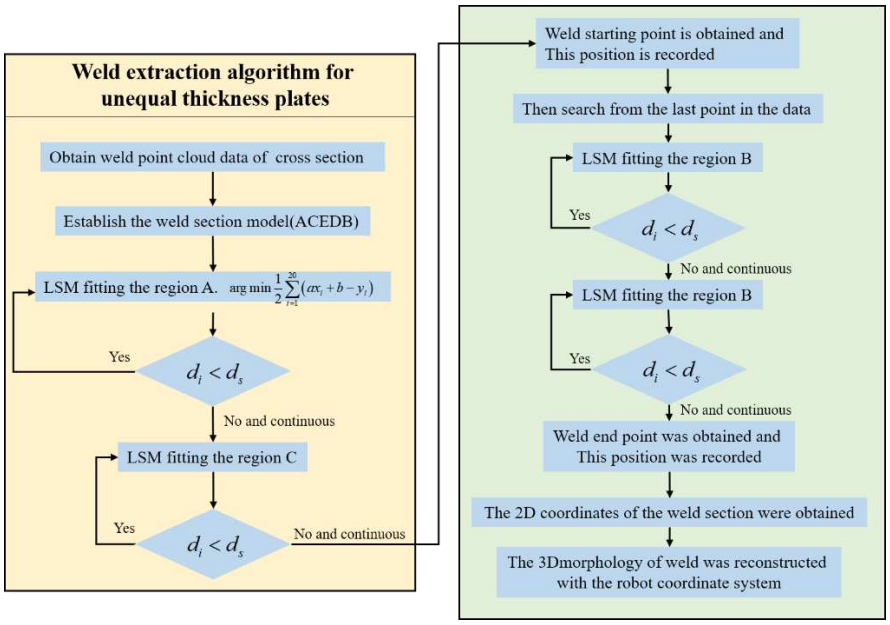

Fig. 6 weld extraction process diagram

The algorithm is aimed at the extraction of welds of steel plates with unequal thicknesses, and its premise is to obtain ordered weld point cloud data, which can be obtained by laser vision sensors based on the principle of triangulation. Firstly, the weld section model is established, and different areas are divided according to the section characteristics. Then the LSM is used to extract the weld contour according to the order of A-C-B-D. In order to accurately extract the weld seam, setting the appropriate threshold d_s is the key. Whether the threshold value is too large or too small will affect the judgment of the region. Therefore, before the actual grinding, we find the right d_s by experiment.

4 groups of weld cross section data were obtained randomly, and d_s were preliminarily set as (0.05, 0.15, 0.25) to process the above 4 groups of data. The extraction effect is shown in the figure below.

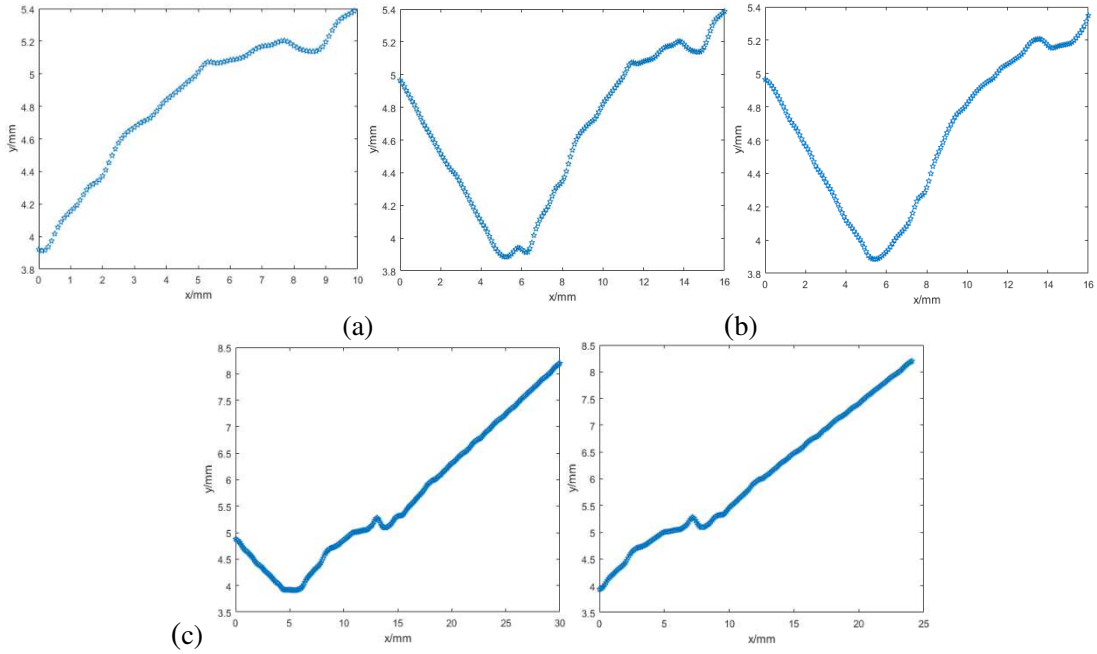

Fig .7 the extraction effect diagram. (a) actual weld profile; (b)-(e) weld profile extracted by experiments (d_z =0.05)

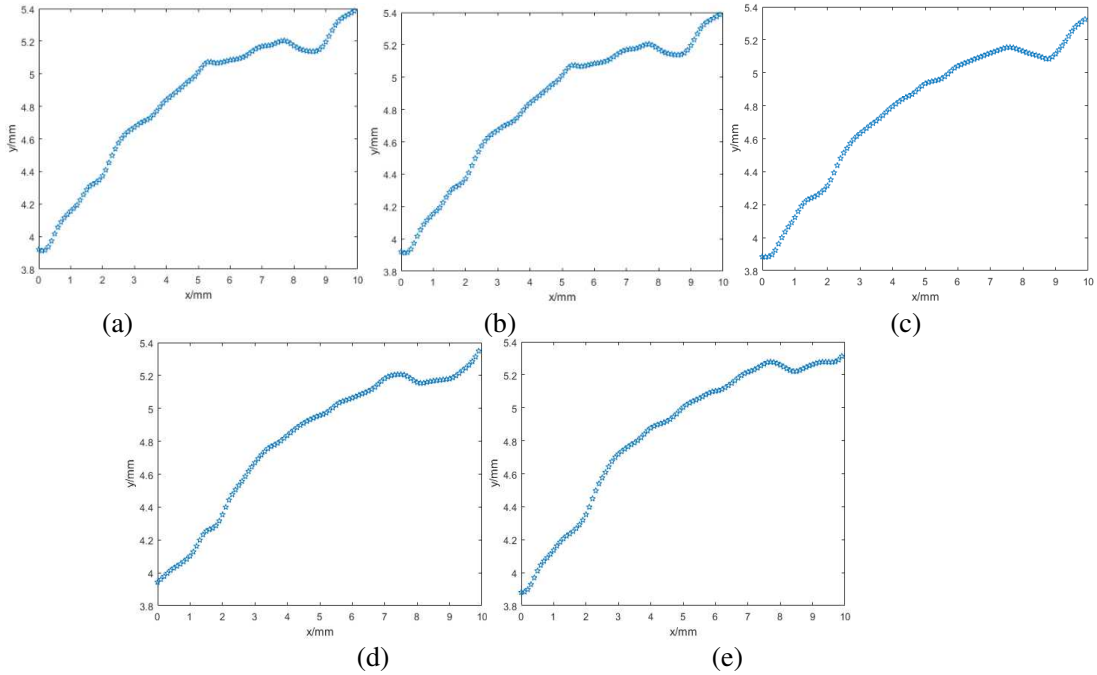

Fig .8 the extraction effect diagram. (a) actual weld profile; (b)-(e) weld profile extracted by experiments (d_z = 0.15)

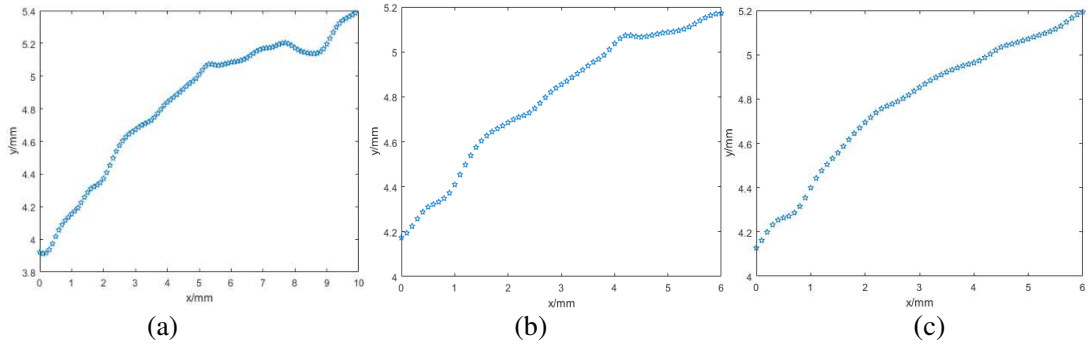

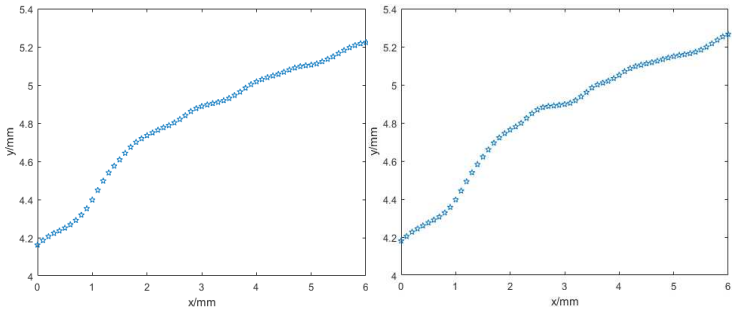

(d) (e)

Fig .9 the extraction effect diagram. (a) actual weld profile; (b)-(e) weld profile extracted by experiments (d_z=0.25)

It can be seen from the experimental results that the size of the threshold has a greater impact on the accuracy of weld extraction. When the threshold value is small (see Fig. 7), it is easy to misjudge areas C and D, resulting in failure to extract the weld contour. When the threshold value is large (see Fig. 9), it is difficult to accurately judge the starting and ending point of the weld, which affects the accuracy of the weld extraction. According to the experimental results, the extraction accuracy is high when d_z=0.15 (see Fig. 8).

3.3 Feature information extraction

To achieve better grinding effect, the height, width and normal vector of the weld seam need to be further obtained. In this paper, the width value and height value are further processed on the basis of the above extraction. The value of each section is saved, and the characteristic information of the entire weld is obtained by combining with the robot position. The process can be expressed as follows.

1 The starting and ending position $p_1(x_1, y_1), p_2(x_2, y_2)$ of the weld seam is obtained.

2 The distance between p_1 and p_2 is calculated to obtain the weld width value according to Eq. (4)

$$D_w = \sqrt{(x_1 - x_2)^2 + (y_1 - y_2)^2} \tag{4}$$

3 The least square method is used to fit the polynomial according to the starting and ending points p_1, p_2.

4 The distance from the point to the polynomial is calculate by Point-by-point search.

5 The maximum distance is found to obtain the weld height data (see Fig.10)

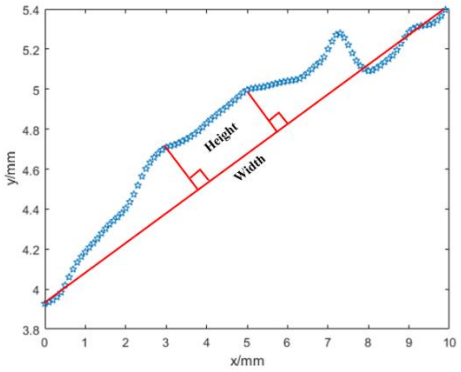

Fig. 10 weld seam feature calculation

4. Grinding path planning

4.1 grinding path fitting

In order to ensure good grinding quality, the grinding must be smooth to avoid the vibration caused by the discontinuous speed and acceleration of the robot. The traditional trajectory fitting methods include 3th degree polynomial fitting [28] and the 5th degree polynomial fitting [29], which have low fitting accuracy and are only suitable for simple trajectory planning tasks. In this paper, the U-direction used a spline function to fit the grinding trajectory based on the obtained weld profile, expressed as Eq. (5). In the actual machining process, the grinding step in U-direction is obtained by the isometric method. Under the condition of ensuring the grinding efficiency and accuracy at the same time, it is more appropriate to set the step as 15mm based on experimental experience.

$$C(u) = \sum_{i=0}^{n} N_{i,k}(u) P_i, 0 \le u \le 1 \tag{5}$$

Where $C(u)$ is a vector function of the B-spline curve, $N_{i,k}(u)$ is the k order spline basis function, which can be obtained by Eq. (6-7) P_i is the known feature point, u is the sequence of

parameters.

$$N_{i,k}(u)=\frac{u-u_i}{u_{i+k}-u_i}N_{i,k-1}(u)+\frac{u_{i+k+1}-u}{u_{i+k+1}-u_{i+1}}N_{i+1,k-1}(u) \quad (6)$$

$$N_{i,0}(u)=\begin{cases}1, & u_i,, u<u_{i+1}\\ 0, & \text{else}\end{cases} \quad (7)$$

In the V-direction, to ensure the smoothness of the grinding surface, The step distance is determined by the equidistant method according to the width of the grinding wheel.

4.2 End pose calculation

The end pose of the robot is a key factor affecting the quality of grinding. Firstly, the pose of weld seam is calculated and the normal vector is obtained. Then the pose of end grinding wheel is adjusted.

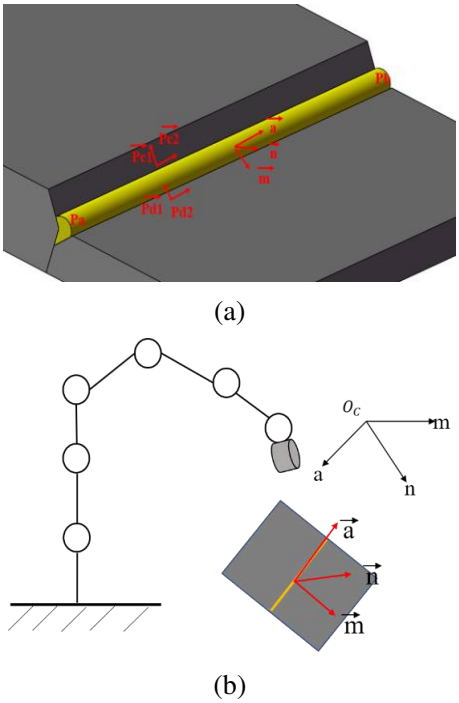

(a) Welding seam normal vector calculation; (b) Robot end pose calculation. Fig. 11 The pose model of weld seam.

The pose model of weld seam is established in Fig 12, which include direction vectors, normal vectors and proximity vectors. The starting and end points $P_a(x_a,y_a,z_a)$, $P_b(x_b,y_b,z_b)$ have been obtained, then the direction vector can be written as Eq. (8)

$$\vec{a}=\frac{\frac{df_x}{d_t}i+\frac{df_y}{d_t}j+\frac{df_z}{d_t}k}{\left\|\frac{df_x}{d_t}i+\frac{df_y}{d_t}j+\frac{df_z}{d_t}k\right\|} \quad (8)$$

$$\vec{m}=(\vec{p}_{c1}-\vec{p}_{c2})\times(\vec{p}_{d1}-\vec{p}_{d2}) \quad (9)$$

$$\vec{n}=\vec{m}\times\vec{a} \quad (10)$$

Where $\vec{m}$ is the proximity vector, $\vec{n}$ is the normal vector.

According to D-H method, six joint coordinate systems of robot were constructed, and the end -tool coordinate system {G} and the laser coordinate system {L} were also considered. Then the transformation matrices between adjacent coordinate systems are expressed as ${}^{w}_{1}T、{}^{1}_{2}T、{}^{2}_{3}T、{}^{3}_{4}T、{}^{4}_{5}T、{}^{5}_{6}T、{}^{6}_{G}T、{}^{G}_{L}T$, which can be calculated by Euler angles (see Fig. 13). The end pose of the robot can be calculated by Eq (11-14)

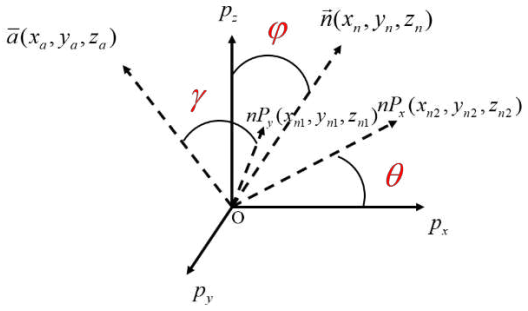

Fig. 12 The pose model of robot end

$$\cos(\theta)=\frac{nP_x\cdot p_x}{|nP_x|\cdot|p_x|}=\frac{x_{n2}\cdot p_x}{\sqrt{x_n^2+y_n^2}} \quad (11)$$

$$\cos(\gamma)=\frac{nP_y\cdot\vec{a}}{|nP_y|\cdot|\vec{a}|}=\frac{x_{n1}\cdot x_a+x_{n2}\cdot y_a+x_{n3}\cdot z_a}{\sqrt{x_{n1}^2+y_{n1}^2+z_{n1}^2}\cdot\sqrt{x_a^2+y_a^2+z_a^2}} \quad (12)$$

$$\cos(\varphi)=\frac{\vec{n}\cdot P_z}{|\vec{n}|\cdot|P_z|}=\frac{z_a\cdot P_z}{\sqrt{x_n^2+y_n^2+z_n^2}\cdot|p_z|} \quad (13)$$

$${}^{W}_{G}T={}^{w}_{1}T\cdot{}^{1}_{2}T\cdot{}^{2}_{3}T\cdot{}^{3}_{4}T\cdot{}^{4}_{5}T\cdot{}^{5}_{6}T\cdot{}^{6}_{G}T \quad (14)$$

Where {W} is world coordinate system. p_x,p_y,p_z are robot base coordinate system, nP_x is the projection of $\vec{n}$ onto the plane p_xop_y. np_y is the projection of $\vec{n}$ onto the plane p_zop_y. θ,γ,φ are Euler angles, which is used to adjust the posture. Before the robot grinding, the transformation relationship between coordinate system{L}and coordinate system{W}is calculated by welding direction vector and normal vector, the end pose is adjusted by hand-eye calibration. The

calculation process of the above trajectory and pose is obtained by MATLAB calculation and realized by OrageEdit programming.

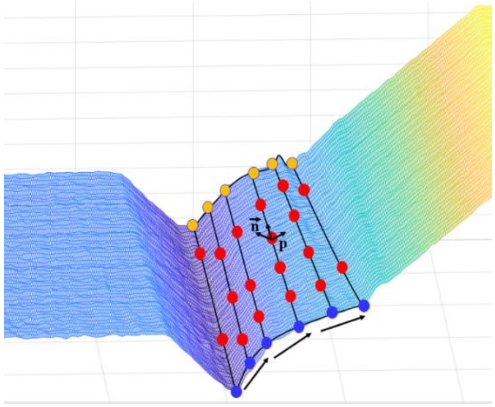

Fig. 13 robot path planning diagram

5. Experiment

5.1 experimental platform

In order to verify the effectiveness of the proposed method, The team built a grinding platform based on KUKA robot [30] (see Fig. 1). The platform integrates weld extraction and automated grinding systems according to proposed method. The platform specifically included KUKA KR210R2700 industrial robot, Keyence LJ-G500 sensor, Self-made flexible support, Industrial PC, SEW company MTA11A-503-S623-D01-00 inverter, AC motor DRE 100M2/FL/LN motor, Siemens SCALAVCEX108poE switches, grinding wheel, force sensor, etc. The experimental part was completed on this platform.

5.2 weld extraction experiment

To verity the effectiveness of the welding seam extraction and reconstruction method, feature extraction experiments are carried out on the welds of unequal-thickness steel plates. As shown in Fig.14(a), the width and height values are obtained with vernier calipers at 5 different positions. The feature data are extracted by model segmentation algorithm and compared with the actual values. In order to evaluate the accuracy of the algorithm, 5 extraction experiments are carried out at 5 different positions (see Fig.14(c), Fig.14(d)). It is found that the error range of the extraction width is ($\pm 0.7mm$-$\pm 1.4mm$), and the error range of height is ($\pm 0.15mm - \pm 0.5mm$) by calculating the experimental average value of each position. The reason for the large width error is that the boundary of the weld is not obvious due to external environmental factor, but the extraction results can basically meet the error requirements. Finally, the extracted weld data was stored in the cache area to reconstruct the three-dimensional morphology of the weld. The reconstruction results are shown in the Fig,14(b)

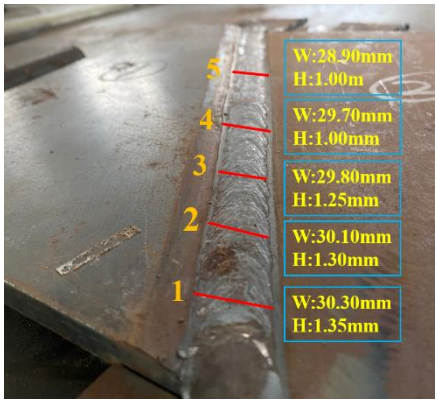

(a)

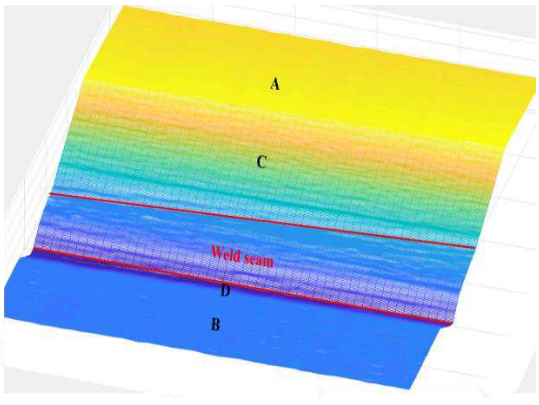

(b)

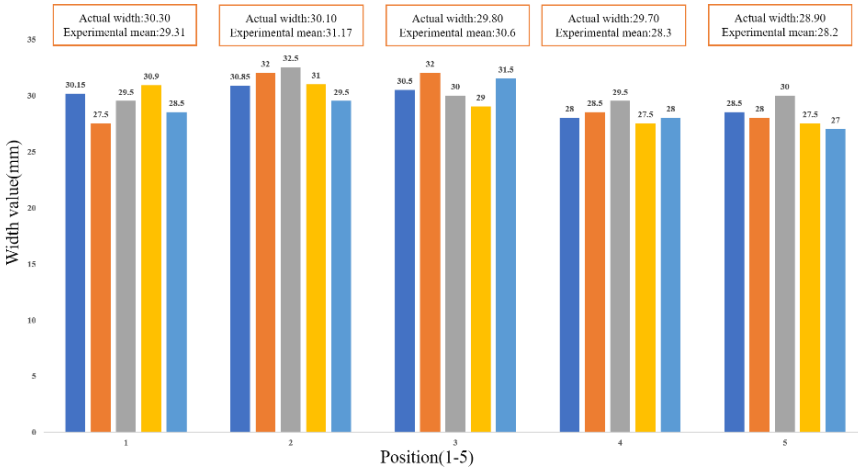

(c)

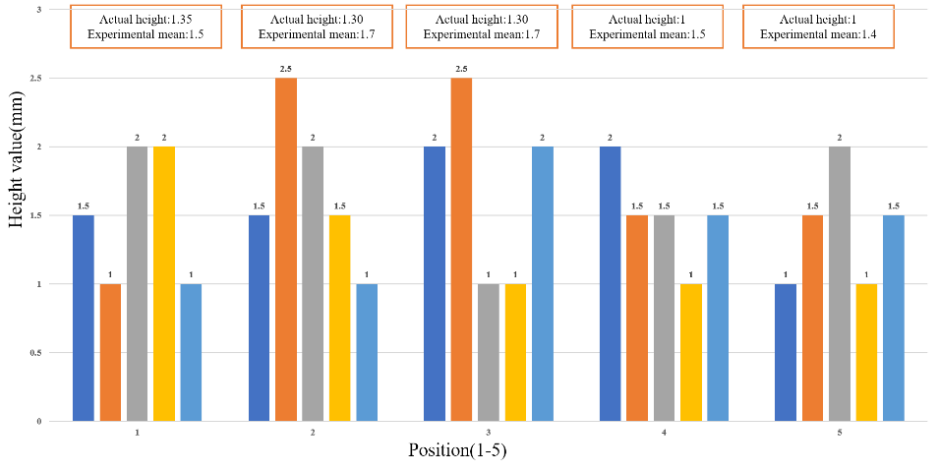

(d)

(a) unequal thickness steel plate weld; (b) 3D reconstruction; (c)weld width extraction; (d)weld height extraction;

Fig. 14 Feature extraction.

5.3 system grinding quality experiment

Weld grinding experiments were carried out based on the above methods of weld extraction and trajectory planning. The grinding track and pose were calculated by MATLAB, and the robot grinding trajectory was programmed in OrageEdit. The grinding effect is shown in the Fig. 15(a) and the roughness result is shown in Fig. 15(c). The average surface roughness is 0.383um after fine grinding. Fig.15(c) shows that due to the instability of grinding starting point, the roughness value at the initial position is relatively high, which reaching 0.555um. Experiments show that the system can fully meet the accuracy requirements.

(a) (b) (c)

(a) surface after grinding; (b) Roughness measuring instrument; (c) Roughness value .Fig.15 grinding effect.

5.4 System Efficiency experiment

In order to test the working efficiency of the system, the grinding experiment is carried out in the traditional way and the method introduced in this article through the welds of two structural parts with the same material, length(60cm) and shape. The grinding time is recorded under the same grinding parameters. The traditional teaching method has low efficiency and poor quality due to complicated procedures and large teaching errors, which takes 7 minutes to grind. The grinding effect is shown in the Fig. 16(a). The system guarantees the polishing quality and improves the polishing efficiency through accurate and efficient welding seam extraction and path planning methods, which only takes 3 minutes to grind. The grinding effect is shown in the Fig. 16(b)

(a) (b)

(a) traditional way for grinding; (b) The system for grinding. Fig. 16 Grinding efficiency experiment.

6 Conclusion

In order to achieve high-quality and efficient welding seam grinding, a simple and effective method of welding seam feature extraction and three-dimensional reconstruction is proposed. A robot automatic welding seam grinding system is built to solve a series of problems in manual grinding. The experimental results prove that the system is reliable and efficient. it has good robustness to complex environments. The main results of this paper are as follows:

1. A new type of flexible bracket structure for weld seam feature extraction is designed, which can ensure that the laser moves with the robot and is projected to the weld surface at any angel. Based on this, a grinding system and laser sensor system are integrated at the end of the robot to build a robot weld automatic polishing platform. The system is efficient and reliable, and has strong engineering significance.

2. A simple and effective method of welding seam feature extraction is proposed. The model classification method based on the least square method is used to extract the weld contour, the problem of processing 3D point cloud data is converted into the problem of processing 2D data, and a data buffer is established to reconstruct the 3D weld.

3. The mathematical model of the weld surface was established, and the attitude angle of the robot end grinding was calculated based on the reconstructed 3D surface of the weld seam. The spline curve method and chord height error method were used to plan the grinding path in U and V directions, which ensured the integrity of the grinding surface.

Declarations

Funding

This work was supported by the municipal joint Fund for Natural Science of Hunan Provincial (Grant number 2021JJ50116). The Special Fund for the Construction of Hunan Innovative Province (Grant number. 2020GK2003). The General project of Hunan Provincial Education Department, China (Grant number. 20C0830).

Conflicts of Competing Interest

We confirm that there are no known conflicts of interest associated with this publication and there has been no significant financial support for this work that could have influenced its outcome.

Ethical approval

We confirm that the manuscript has not been submitted to any other journal. The submitted work is original and has not been published elsewhere in any form or language.

Consent to participate

We confirm that all authors agree with the content and give explicit consent to submit

Consent for publication

If the article is accepted, we grant the Publisher an exclusive licence to publish the article.

Availability of data and material

We confirm that data is open and transparent

Code availability

Not applicable.

Authors' contributions

Jimin Ge: **Conceptualization** Investigation, Writi ng-original draft, Writing-review & editing.
Zhaohui Deng: Writing-review & editing, Fundi ng ac- quisition.
Zhongyang Li: Writing-review & editing.
Wei Li: Writing-review & editing.
Tao Liu review & editing.
Hua Zhang: Funding acquisition.
Jiaxu Nie: review & editing

References

[1] Zhu Y, Mu W, Cai Y, Xin D, Wang M. A novel high-efficient welding technology with rotating arc assisted by laser and its application for cryogenic steels[J]. Journal of Manufacturing Processes, 2021, 68: 1134-1146.

[2] Baicun W. Jack HS, Lei S, Theodor F. Intelligent welding system technologies: State-of-the-art review and perspectives[J]. Journal of Manufacturing Systems, 2020, 56: 373-391.

[3] Moritz B, Xiru W. A review of fatigue test data on weld toe grinding and weld profiling[J]. International Journal of Fatigue, 2020: 106073.

[4] Fu Z, Ji B, Kong X, Chen X. Grinding treatment effect on rib-to-roof weld fatigue performance of steel bridge decks[J]. Journal of Constructional Steel Research, 2017, 129: 163-170.

[5] Wang Q, Wang W, Zheng L, Yun C. Force control-based vibration suppression in robotic grinding of large thin-wall shells[J]. Robotics and Computer-Integrated Manufacturing, 2021, 67: 102031.

[6] Zhu D, Feng X, Xu X, Yang Z, Li W, Yan S, Ding H. Robotic grinding of complex components: a step towards efficient and intelligent machining–challenges, solutions, and applications[J]. Robotics and Computer-Integrated Manufacturing, 2020, 65: 101908.

[7] Lin F, Lv T. Development of a robot system for complex surfaces polishing based on CL data[J]. The International Journal of Advanced Manufacturing Technology, 2005, 26(9-10): 1132-1137.

[8] Bedaka AK, Lin CY. CAD-based robot path planning and simulation using OPEN CASCADE[J]. Procedia computer science, 2018, 133: 779-785.

[9] Comas T, Diao C, Ding L, Williams S, Zhao Y. A passive imaging system for geometry measurement for the plasma arc welding process[J]. IEEE Transactions on Industrial Electronics, 2017, 64(9): 7201-7209.

[10] Wu C, Gao J, Liu X, Zhao Y. Vision-based measurement of weld pool geometry in constant-current gas tungsten arc welding[J]. Proceedings of the institution of mechanical engineers, Part B: Journal of Engineering Manufacture, 2003, 217(6): 879-882.

[11] Charrett T, Bandari Y, Michel F, Ding J, S Williams. A non-contact laser speckle sensor for the measurement of robotic tool speed[J]. Robotics and Computer-Integrated Manufacturing, 2018, 53: 187-196.

[12] Huang S, Niklas B, Yamakawa Y, Senoo T, M Ishikawa. Robotic contour tracing with high-speed vision and force-torque sensing based on dynamic compensation scheme[J]. IFAC-Papers On Line, 2017, 50(1): 4616-4622.

[13] Wang Y, Ding W, Mei D. Development of flexible tactile sensor for the envelop of curved robotic hand finger in grasping force sensing[J]. Measurement, 2021,

180: 109524.

[14] Segreto T, Karam S, Teti R, J Ramsing. Feature extraction and pattern recognition in acoustic emission monitoring of robot assisted polishing[J]. Procedia CIRP, 2015, 28: 22-27.

[15] Wang N, Zhong K, Shi X, Zhang X. A robust weld seam recognition method under heavy noise based on structured-light vision[J]. Robotics and Computer-Integrated Manufacturing, 2020, 61: 101821.

[16] Liu J, Fan Z, Olsen S, K Christensen, J Kristensen. Boosting active contours for weld pool visual tracking in automatic arc welding[J]. IEEE Transactions on Automation science and engineering, 2015, 14(2): 1096-1108.

[17] Xu Y, Fang G, Lv N, Chen S, Zou J. Computer vision technology for seam tracking in robotic GTAW and GMAW[J]. Robotics and computer-integrated manufacturing, 2015, 32: 25-36.

[18] Ye Z, Fang G, Chen S, Dinham M. A robust algorithm for weld seam extraction based on prior knowledge of weld seam. Sens Rev, 2013,(33):125–33.

[19] Xu Y, Yu H, Zhong J, Tao L, Chen S. Real-time seam tracking control technology during welding robot GTAW process based on passive vision sensor[J]. Journal of Materials Processing Technology, 2012, 212(8): 1654-1662.

[20] Xue K, Wang Z, Shen J, Zhen Y, Liu J, Wu D, Yang H. Robotic seam tracking system based on vision sensing and human-machine interaction for multi-pass MAG welding[J]. Journal of Manufacturing Processes, 2021, 63: 48-59.

[21] Xiao R, Xu Y, Hou Z, Chen C, Chen S. An adaptive feature extraction algorithm for multiple typical seam tracking based on vision sensor in robotic arc welding[J]. Sensors and Actuators A: Physical, 2019, 297: 111533.

[22] Yang L, Liu Y, Peng J, Liang Z. A novel system for off-line 3D seam extraction and path planning based on point cloud segmentation for arc welding robot[J]. Robotics and Computer-Integrated Manufacturing, 2020, 64: 101929.

[23] Huang W, Kovacevic R. Development of a real-time laser-based machine vision system to monitor and control welding processes[J]. The International Journal of Advanced Manufacturing Technology, 2012, 63(1): 235-248.

[24] Shao W, Huang Y, Zhang Y. A novel weld seam detection method for space weld seam of narrow butt joint in laser welding[J]. Optics & Laser Technology, 2018, 99: 39-51.

[25] Zhang L, Ye Q, Yang W, Jiao J. Weld line detection and tracking via spatial-temporal cascaded hidden Markov models and cross structured light[J]. IEEE Transactions on Instrumentation and Measurement, 2013, 63(4): 742-753.

[26] Iakovou D, Aarts R, Meijer J. Sensor integration for robotic laser welding processes[C]//International Congress on Applications of Lasers & Electro-Optics. Laser Institute of America, 2005, 2005(1): 2301.

[27] Ye G, Guo J, Sun Z, Li C, Zhong S. Weld bead recognition using laser vision with model-based classification[J]. Robotics and Computer-Integrated Manufacturing, 2018, 52: 9-16.

[28] Lin C, Chang P, Luh J. Formulation and optimization of cubic polynomial joint trajectories for industrial robots[J]. IEEE Transactions on automatic control, 1983, 28(12): 1066-1074.

[29] Boryga M, Graboś A. Planning of manipulator motion trajectory with higher-degree polynomials use[J]. Mechanism and machine theory, 2009, 44(7): 1400-1419.

[30] Ge J, Deng Z, Li Z, Li W, LV L, Liu T. Robot welding seam online grinding system based on laser vision guidance[J]. The International Journal of Advanced Manufacturing Technology, 2021: 1-13.